Jaesool Shim, Prashanta Dutta*

Joule Heating Effect in Constant Voltage Mode Isotachophoresis in a Microchannel

Abstract: Microchip ITP (isotachophoresis) is getting popularity as a preparative technique for preconcentration and separation of chemical species and/or ions in liquid phase. In constant voltage mode ITP, generally a high electric potential difference is applied to a discontinuous buffer for faster and higher resolution separation. However, the higher current from the applied electric field induces Joule heating in the buffer which modifies the mobility and diffusion coefficient of analytes in the system. This change in mobility and diffusion coefficient strongly influences the transient separation process in ITP. In this study the effect of Joule heating on separation behavior of analyte compounds has been presented in a constant voltage mode ITP where two chemical species are separated from an initial mixture. The model is based on mass, energy, and charge conservation and electroneutrality condition in the system. A set of nonlinear governing equations are solved numerically for temperature dependent properties such as diffusion coefficient, effective electrophoretic mobility, and thermal conductivity using a finite volume based model. Numerical results suggest that for temperature dependent properties of control parameters, the separation speed of analytes is significantly different from that of constant temperature case. In constant voltage mode ITP, the temperature peak forms at the location of trailing electrolyte, and its influence propagates toward the direction of band movement as separation proceeds.

Keywords: Joule heating, isotachophoresis, microchip separation, microfluidic

PACS® (2010). 41.20.Cv, 44.15.+a, 47.11.Df

Jaesool Shim: School of Mechanical Engineering, Yeungnam University, Gyeongsan 712-749, Korea

***Corresponding author: Prashanta Dutta:** School of Mechanical and Materials Engineering, Washington State University, Pullman, WA 99164-2920, USA, E-mail: dutta@mail.wsu.edu

1 Introduction

Isotachophoresis (ITP) is a separation and preconcentration technique suitable for both preparative [1–3] and microchip [4, 5] device to isolate charged biomolecules such as RNA, DNA, protein, etc under the influence of an external electric field. ITP has the advantage over other concentration/separation techniques such as field induced stacking and isoelectric focusing in that it can be performed at virtually any conductivity and pH. Depending on the types of ions separated, ITP can be classified into two sub categories: anionic and cationic. In the anionic ITP negatively charged ions are separated, while the cationic ITP is used to separate positively charged components.

Like any other electrophoretic technique such as zone electrophoresis, capillary electrophoresis, and isoelectric focusing, the temperature rise during an ITP process is expected because of Joule heating. The interaction between applied electric field and ionic components is responsible for the volumetric (Joule) heat generation in an electrolyte system [6–8]. Although Joule heating is a byproduct of any electromigration based separation and concentration process, it can be tuned to design and operate novel separation techniques such as temperature gradient focusing [9, 10] where the analytes are separated in a temperature field under the action of an electric field.

The amount of heat generation due to Joule heating primarily depends on the electric field and the conductivity of the buffer. Since ITP takes place in a discontinuous buffer, the conductivity and electric field vary between two adjacent electrolytes, and hence the amount of heat generation is not a constant throughout the system. Moreover, the heat generation rate increases in ITP if one uses higher potential difference for faster ITP separation. Griffith et al. [11] concluded that an effective cooling system allows a higher potential to be used for faster ITP separation. However, it will not alleviate temperature gradient from one zone to the next, which facilitates the conduction heat transfer between adjacent zones.

ITP is generally used as a preprocessing step as it cannot create a baseline separation, and the target

component(s) are usually transferred to another high-resolution separation column for further separation, manipulation, and/or sensing [12, 13]. Hence the identification of interface location is very important. Often times, the interface location and shape are affected by the axial temperature gradient in the ITP column. Reijenga et al. [14] determined the length of diffusion-controlled layer as a function of temperature in steady-state ITP. The temperature rise also adversely affects the quality of the biological molecules such as DNA and protein. For instance, thermal denaturation of proteins occurs at or above 50 °C, and hence the electric field should be controlled to keep the temperature in ITP column below the critical point to avoid undesirable consequences [15]. Pfeifer et al. [16] determined the optimal working temperature range for ITP experiments to separate phenol from industrial waste water.

Although the effect of temperature in large-scale ITP instrument has been addressed adequately, very little attention has been paid to study temperature dependence in microchip ITP. Lately, on-chip isotachophoresis has received significant attention due to its speed, cost-effectiveness, and low sample consumption [4, 17–19]. Moreover, microchannel based ITP is carried out in free solution rather than in a gel. Hence, this process can handle molecular weights ranging from peptides to large protein complexes or even organelles and whole cells. Thus, understanding the effect of temperature on ITP is very important for the microchip design. Krivtzun et al. [20] measured the temperature of liquids in microchip ITP by contactless optical technique, and they found that the temperature changes from zone to zone as the Joule heat depends on the conductivity of a zone. Later, Koch et al. [21] modified this technique to improve the lower detection limit of optical detection technique so that it could be used to measure temperature in microchip ITP more precisely.

Despite these experimental studies, the lack of fundamental understanding on the effect of temperature in ITP performance and its consequence on separable samples still remain unanswered. It is challenging to study Joule heating effect on the ITP behavior because of the nonlinear dependency among control parameters such as electrophoretic mobility, electric field, conductivity, temperature, etc. Until early 1980's most of the ITP literature was based on experimental and/or simplified theoretical models. In 1983, Bier et al. [22] proposed a full-scale, unified mathematical model for transient electrophoretic separation processes and presented simulation results for zone electrophoresis, moving boundary electrophoresis, isotachophoresis and isoelectric focusing in a circular tube. Fidler et al. [23] described a simplified mathematical model for ITP and obtained simulation results to separate two samples in a capillary tube. In their computer model, diffusion coefficients were ignored to simplify the computational effort. Later, Mosher et al. [24] described a computer model that takes care of diffusional effects for the exact prediction of boundary shape for weak electrolytes. They have also considered the pH effects in the computer model by including hydronium and hydroxyl ions in the ITP model. The effects of co- and counter-flow on ITP transport behavior were predicted by Deshmukh and Bier [25]. More recently, Shim et al. [26] presented a general mathematical model for multi-dimensional electrophoresis for any number of multivalent electrolytes in free solution.

In this study, a multi-dimensional ITP model is developed considering Joule heating effect to study the behavior of the separable samples in a microfluidic channel. In this model, the electrochemical parameters such as diffusion coefficient and electrophoretic mobility of samples and electrical conductivity of the buffer solution are expressed as a function of temperature. Moreover, the dissociation and association relations of components are considered for calculating the effective valence and the pH of the system. Numerical results are presented for ITP with and without the Joule heating contribution to reveal the effect of temperature.

2 Theory

The schematic of a typical ITP process is presented in figure 1 where separation of two sample components is shown. In ITP, sample (target and/or impurities) constituents are initially loaded between a leading electrolyte and a terminating electrolyte (Fig. 1a), and a current is applied to initiate the separation process. For an ITP separation, the electrophoretic mobility of the leading electrolyte and terminating electrolyte should be the highest and the least respectively, while the electrophoretic mobility of sample constituents should be higher than that of a terminating ion and smaller than that of a leading ion for a given pH range. During the initial stages of ITP (Fig. 1b&c), the sample constituents separate and/or concentrate according to their net mobilities and create sharp moving boundaries between the sample constituents. At steady state (Fig. 1d&e), all moving boundaries migrate towards cathode or anode with a constant velocity for cationic and anionic ITP, respectively.

In the past, we have presented a mathematical model for ITP based on mass and charge conservation equations

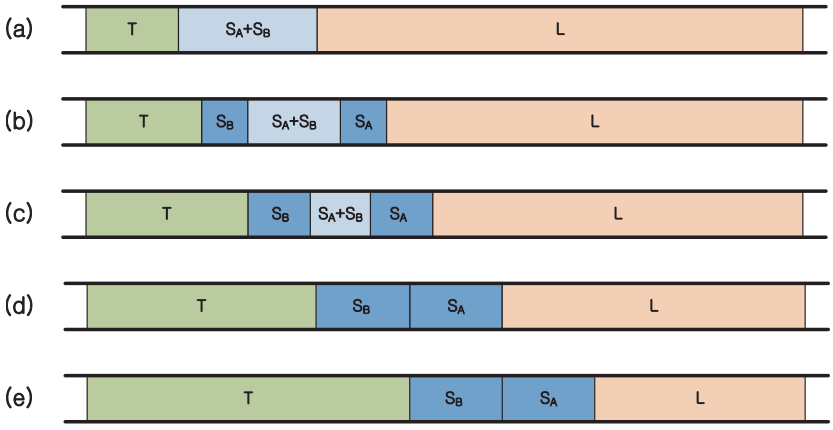

Fig. 1: Schematic of ITP process with two samples (S_A and S_B) showing important characteristics at different time during separation. Initially the samples are mixed and placed between a leader (L) and a terminator (T). The electrophoretic mobility of the leader (μ_L) is the highest, while the electrophoretic mobility of the terminator is the least (μ_T). For separation of sample components, the electrophoretic mobility of the samples should be $|\mu_T| < |\mu_B| < |\mu_A| < |\mu_L|$. For anionic ITP, the anode is at the right end and the cathode is at the left end.

of ionic components [27]. However, in that model the effect of heat generation due to Joule heating was not taken into consideration under the assumption that heat dissipates quickly to the surrounding. This assumption is valid for large laboratory type ITP instrument where a cooling module is also incorporated for quick disposal of Joule heat. But in on-chip ITP, generally no such cooling mechanism is available. Moreover, the substrates (glass, PDMS, PMMA, acrylic) used for housing microchannel are generally made of dielectric materials which are not a good thermal conductor. In other words, in microscale ITP, the internally generated heat cannot leave the system and it increases the temperature of the buffer solution, which essentially affects the performance of ITP separation subsequently. Thus, to account for the effect of temperature in separation behavior, one has to know the temperature distribution in the system.

2.1 Governing equations

The temperature distribution in an electrolyte system subjected to an electric field is governed by the energy equation as [28]

$$\rho C_p\left(\frac{\partial T}{\partial t}+\vec{U}\cdot\nabla T\right)=\nabla\cdot(k\nabla T)+\sigma(\vec{E}\cdot\vec{E}) \tag{1}$$

where t is the time, T is the temperature, ρ is the density of buffer solution, C_p is the specific heat at constant pressure, and $\vec{U}$ and $\vec{E}$ are the flow field and electric field, respectively. k and σ are the thermal and electrical conductivity of the buffer solution which are function of temperature. The electrical conductivity also depends on the concentration of the individual components/electrolytes in the system.

In an ITP system, the concentration of the i^{th} component (C_i) is obtained by summing all J_i+1 species (S_{ij}) in the system with a total of J_i dissociable groups as [26]

$$C_i=\sum_{j=1}^{J_i+1}S_{ij}. \tag{2}$$

Therefore, the mass conservation equation for each component is given as

$$\frac{\partial C_i}{\partial t}+\nabla\cdot[\vec{U}C_i+\langle\mu_i\rangle\vec{E}C_i-D_i\nabla C_i]=0, \tag{3}$$

where D_i is the diffusion coefficient of component i. The effective mobility ($\langle\mu_i\rangle$) of a component can be defined as

$$\langle\mu_i\rangle=\frac{\sum_{j=1}^{J_i+1}\mu_{ij}S_{ij}}{C_i}=\frac{\sum_{j=1}^{J_i+1}z_{ij}\omega_{ij}S_{ij}}{C_i}. \tag{4}$$

If the dissociation reactions are fast, we also have J_i algebraic relations for equilibrium constants (K_{ij}) among the component i species,

$$K_{ij}=\frac{C_{H^+}S_{ij}}{S_{ij+1}} \tag{5}$$

which must be solved together with mass conservation for each component. The relations between components and their associated species are [26]

$$C_i = S_{ij}\left(1+\sum_{jj=1}^{J_i}\prod_{k=1}^{jj}\frac{C_{H^+}}{K_{ik}}\right) \quad \text{if } j=1,$$

$$= S_{ij}\left(\prod_{k=1}^{j-1}\frac{K_{ik}}{C_{H^+}}\right)\left(1+\sum_{jj=1}^{J_i}\prod_{k=1}^{jj}\frac{C_{H^+}}{K_{ik}}\right) \quad \text{if } j\geq 2. \tag{6}$$

For a system with M components, the charge conservation equation can be expressed as

$$\nabla\cdot[\sigma E] = F\left(\sum_{i=1}^{M}\sum_{j=1}^{J_i+1} z_{ij}D_{ij}\nabla^2 S_{ij} + D_{H^+}\nabla^2 C_{H^+} - D_{OH^-}\nabla^2 C_{OH^-}\right)$$

$$- FU\left(\sum_{i=1}^{M}\sum_{j=1}^{J_i+1} z_{ij}S_{ij} + C_{H^+} - C_{OH^-}\right). \tag{7}$$

The electrical conductivity (σ) can be expressed as

$$\sigma = F\left[\sum_{i=1}^{M}\sum_{j=1}^{J_i+1} z_{ij}\mu_{ij}S_{ij} + (\mu_{H^+}C_{H^+} - \mu_{OH^-}C_{OH^-})\right] \tag{8}$$

where F is the Faraday constant. The concentration of the hydronium (H^+) can be estimated from the electroneutrality constraint as,

$$C_{H^+} - \frac{K_W}{C_{H^+}} = -\sum_{i=1}^{M}\langle z_i\rangle C_i \tag{9}$$

where K_W is the equilibrium constant for water.

Note that the temperature dependent ITP model presented here is fully coupled as the thermal conductivity (k), electrical conductivity (σ), diffusion coefficient (D), and electrophoretic mobility (ω) are function of temperature. Hence their values need to be updated before solving mass, charge and energy conservation equations, and an iterative scheme will be used to solve them.

3 Numerical model

3.1 Assumptions

The main simplifying assumptions and approximations are as follows:

i. Thermodynamic properties such as density (ρ), and specific heat capacity (C_p) of buffer solution are weak function of temperature, and hence they are assumed constant in our numerical simulation.
ii. In computing temperature distribution from the energy equation, the density, heat capacity, and thermal conductivity of water are used because the concentration of solutes is very low in our model system.
iii. The contribution of advection term is neglected where there is no counter (bulk) flow.
iv. The electric field-induced electroosmotic flow is not considered here either because, in most ITP experiments, the channel is dynamically coated with chemicals to suppress electroosmosis.
v. The anodic and cathodic reservoirs are assumed to be much larger than the microchannel to maintain constant fluid temperature at the entry and exit of the ITP channel.
vi. The buffer solution is considered to be an incompressible fluid, and no adsorption and permeation of sample solutes take place onto the microchannel walls and reservoirs.
vii. The absolute mobility of ionic species is not a strong function of ionic concentration.

3.2 Initial and boundary conditions

The initial distribution of electrolytes is very important in ITP. In this study, a mixture of two components (Sample A and B) is initially placed between a leader and a terminator. Here hydrochloric acid and caproic acid are used as leader and terminator respectively, while the acetic acid and benzoic acid are chosen as Sample A and B. Moreover, the histidine is used as a counter ion for electroneutrality in the system. The initial distributions of all components are shown in Figure 2 (top). In solving mass conservation equations, the net flux through the channel walls and end wells (reservoirs) are set to zero. For the energy equation, adiabatic condition ($\nabla T\cdot\vec{n}=0$) is maintained at the channel wall, and a constant temperature value is imposed at the anodic and cathodic wells. Similarly, for the charge conservation equation, the electric potential is subjected to insulating boundary conditions ($\nabla\phi\cdot\vec{n}=0$) on the walls, and Dirichlet boundary conditions are applied at the electrode (end) wells. The value of electric potential at the anode is varied from case to case, while the cathode is maintained at the ground. Initial temperature as well as the electrode temperature are kept constant at $T = 298$ K.

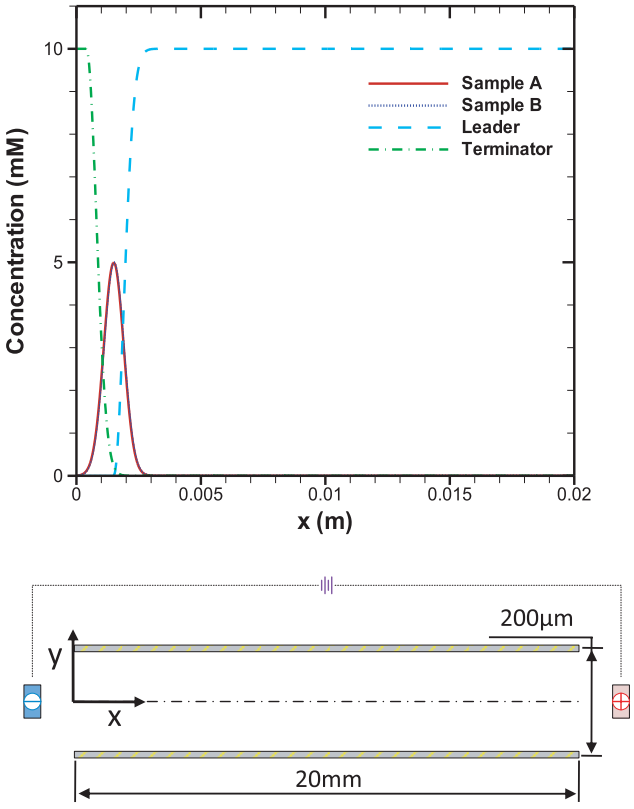

Fig. 2: (Top) Initial concentration distributions for all five ionic components used in the ITP simulation and (bottom) schematic of the computational domain.

3.3 Numerical scheme

In this study, a finite volume based numerical method [29] is used for the ITP problem. Discretized algebraic equations are obtained at each grid point for the mass conservation, energy conservation and charge conservation equations. For the computational simplicity and stability, structured grids are considered in the simulation. The tri-diagonal matrix algorithm is used to solve the discretized algebraic equations along a grid line, and a line by line iteration is employed until converged results are obtained throughout the computational domain [29]. The convergence criteria are set as $\left|\frac{C_n - C_{n-1}}{C_n}\right| \leq 10^{-5}$, $\left|\frac{\phi_n - \phi_{n-1}}{\phi_n}\right| \leq 10^{-5}$ and $\left|\frac{T_n - T_{n-1}}{T_n}\right| \leq 10^{-5}$ for mass conservation, charge conservation and temperature equation, respectively. The subscript (n) and $(n-1)$ denote the current and previous iteration step. To validate the numerical model, our numerical results are compared with existing literature [30] for no Joule heating case, and an excellent agreement is obtained between them.

4 Results and discussion

Numerical results for temperature dependent ITP are obtained in a two-dimensional (2 cm long and 200 micron wide) straight microchannel (Figure 2(bottom)). Although our numerical model is capable of solving three-dimensional problems to capture the transient dynamics during the ITP process, a 2D model is suffice here as the contribution of the bulk flow is neglected in the model problem. ITP without bulk flow eliminates the dependency in the channel height direction. Five different components, leader, terminator, Sample A, Sample B, and a counter ion, are considered in this numerical simulation, though more sample components can be added without modifying the current mathematical and numerical models. The physicochemical properties of these 5 ionic components are shown in Table 1. The density and specific heat capacity for the buffer solution are set as 998 $\frac{kg}{m^3}$ and 4.18 $\frac{kJ}{Kg \cdot K}$. The temperature dependent functions for solute electrophoretic mobility ($f(T)$) and buffer thermal conductivity ($g(T)$) are presented in Table 2. The Nernst-Einstein equation $\left(D_i = \frac{RT\omega_i}{F}\right)$ is used to calculate the diffusion coefficient from the absolute mobility, where R is the gas constant and T is the absolute temperature. We specifically study the influence of temperature dependent properties such as thermal conductivity, diffusion coefficient, electrophoretic mobility, and electrical

Type	Component	pK_1	pK_2	pK_3	ω (10E-9 m²/Vs)
Leader (L)	Hydrochloric acid	−2.00	–	–	79.1
Terminator (T)	Caproic acid	4.857	–	–	30.2
Sample A	Acetic acid	4.756	–	–	42.4
Sample B	Benzoic acid	4.203	–	–	33.6
Counter ion	Histidine	2.000	6.04	9.33	28.8

Table 1: Physicochemical properties of different components. The maximum charge state of leader, terminator, sample component A and sample component B is −1, but that for the counter ions is +2. The initial temperature is 25 °C.

Properties	Expression	Temperature correction
$\omega_i(T)$	$\omega_i(T) = \omega_0(T) f(T)$	$f(T) = 1 + 0.02(T - T_\infty)$
$K(T)$	$k(T) = k_0\, g(T)$	$g(T) = 0.61 + 0.0012(T - T_\infty)$

Table 2: Expression for the temperature dependent functions of electrophoretic mobility (ω_i) and thermal conductivity (k). The temperature correction functions are obtained from [33, 34]. The reference temperature T_∞ is 25 °C.

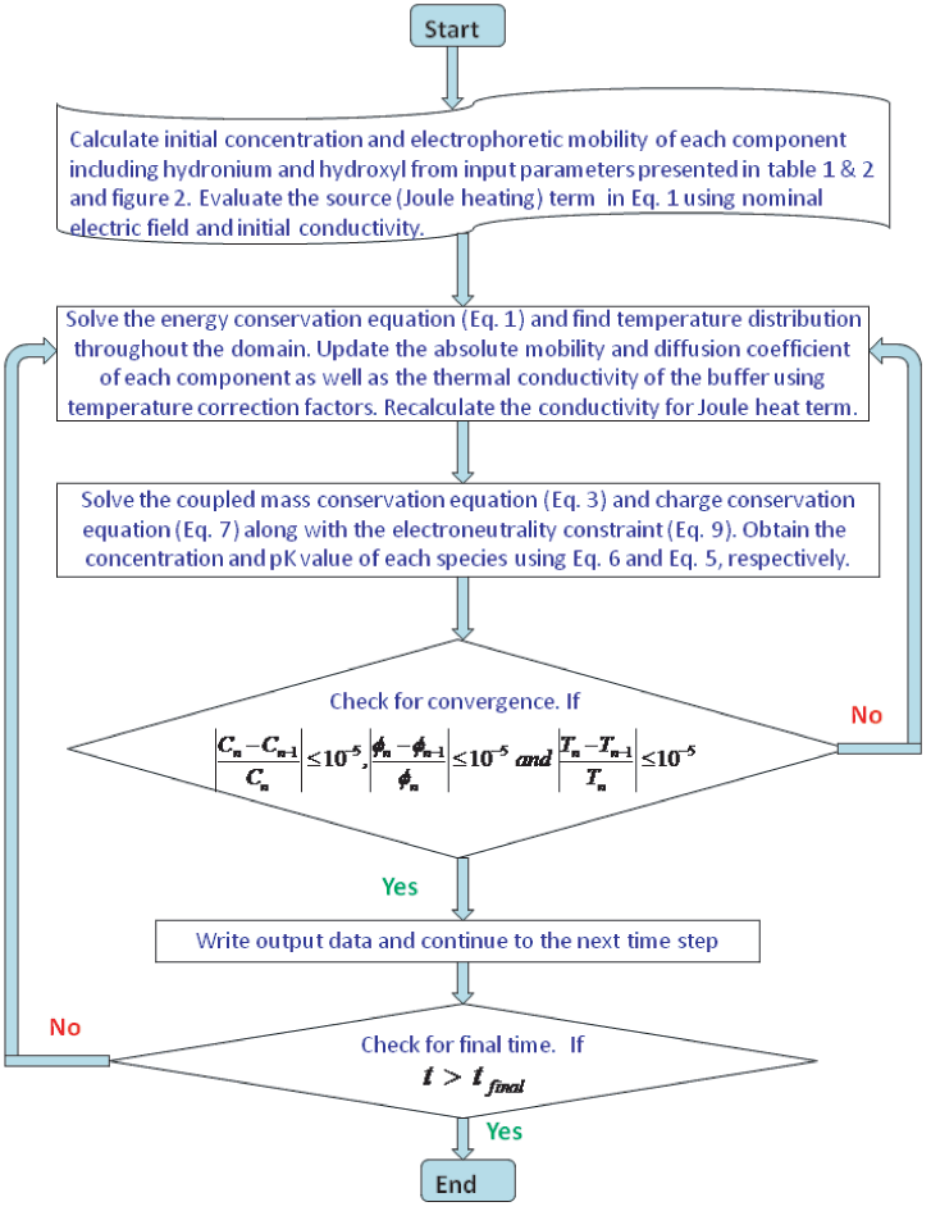

Fig. 3: Algorithm used to solve the coupled mass, charge and energy conservation equations presented in the mathematical model for temperature dependent ITP.

conductivity on the isotachophoretic separation characteristics. The temperature dependent electrophoretic mobility (μ_i) is calculated from effective valance ($\langle z_i \rangle$) obtained from the pK values of a component and time dependent absolute mobility (ω_i). The details of the calculation procedure are shown in figure 3.

Figure 4 shows the transient separation behavior of ITP for an anode and a cathode potential of 100 V and 0 V,

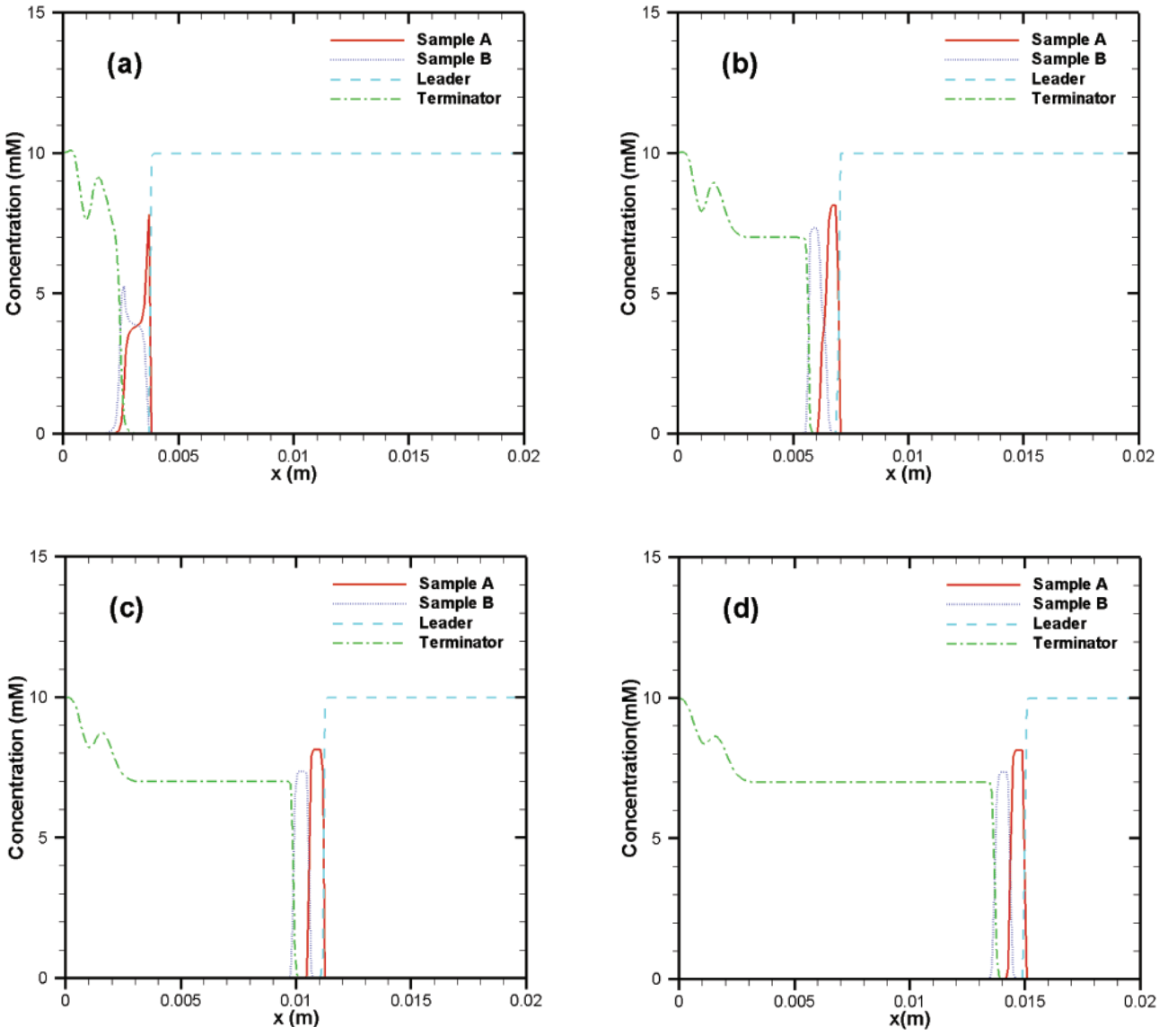

Fig. 4: Concentration distributions of different components along a straight microchannel at (a) 5 s, (b) 15 s, (c) 30 s and (d) 45 s. The anode potential is 100 V and the cathode potential is 0 V. Joule heating contribution is considered by solving the energy equation at each time step and updating all properties based on the temperature before solving mass conservation, charge conservation, and electroneutrality equations. All simulation conditions are shown in Table 1 and 2.

respectively. Joule heating due to the applied electric field is considered in the numerical results. During the initial stages of separation (Fig. 4a), sharp boundaries are formed between the sample A & the leader and the sample B & the terminator. This is a hallmark behavior of ionic components at the early stage of an ITP separation. As the separation progresses, all components move to the right direction, albeit at different velocity, and the overlapped region of two samples is reduced as shown in Fig. 4b. At steady states (Fig. 4(c–d)), both sample A and B form stable concentration profiles, and these bands move towards the anode at a constant velocity. It is important to note that ITP cannot form baseline separation even at the steady state. Rather two consecutive bands maintain minor overlap. The amount of overlap can be controlled by manipulating the applied electric field or the electrophoretic mobility of the components. However, the overlap region cannot be eliminated. Another important aspect of ITP, as shown in figure 4, is the amplification ability where the concentrations of the sample component A and B have been increased by a factor of 1.63 and 1.47, respectively. For the case shown in figure 4, no further amplification is possible as the ITP reached plateau mode. In a peak mode ITP, the amplification factor can be

improved further by changing the channel cross section area [5, 19] and/or applying higher electric field. Higher electric field also speeds up the ITP separation process. As seen from figure 4, with a nominal electric field of 50 V/cm, ITP can be completed in less than a minute due to the much shorter length scale of microfluidic device, while it takes 100 sec and 120 sec for a nominal electric field of 37.5 and 25 V/cm (not shown).

The comparison of separation behavior with and without Joule heating effect is shown in figure 5. At the early stage of ITP ($t = 5$ sec), the separation behavior is almost identical for both cases. This means that the effect of temperature is not strong enough to make an appreciable change in the behavior of sample components. But the numerical results suggest that the speed of sample movement is much faster at later time (15 to 45 sec) if Joule heating is considered into the model. For instance, the nominal speed of sample A is 233 μm/s without joule heating, while it is about 244 μm/s with joule heating. This is due to the fact the Joule heating raises the temperature of the buffer which in turn increases the electrophoretic mobility of the sample component. However, as seen from the Fig. 5, the height and width of the focused band does not get affected by the temperature rise. Nevertheless, the effect of temperature is very significant in the separation behavior, and one has to take this into consideration for the sample transfer process to the next separation dimension. Figure 6 shows the error in band location if the Joule heating effect is not considered in the model. During the initial stage of separation, the minor differences in the band shift between sample A and B are due to the differential velocity of component A and B. Not surprisingly, at steady state, the error is exactly same for both sample A and B because the same correction factor was used for mobility of both components. In reality these temperature correction factors might be different and the results of the separation process will also be different.

The temperature distribution along the channel is shown in Figure 7 for three different applied anode electric potentials. Selection of this anode electric potential

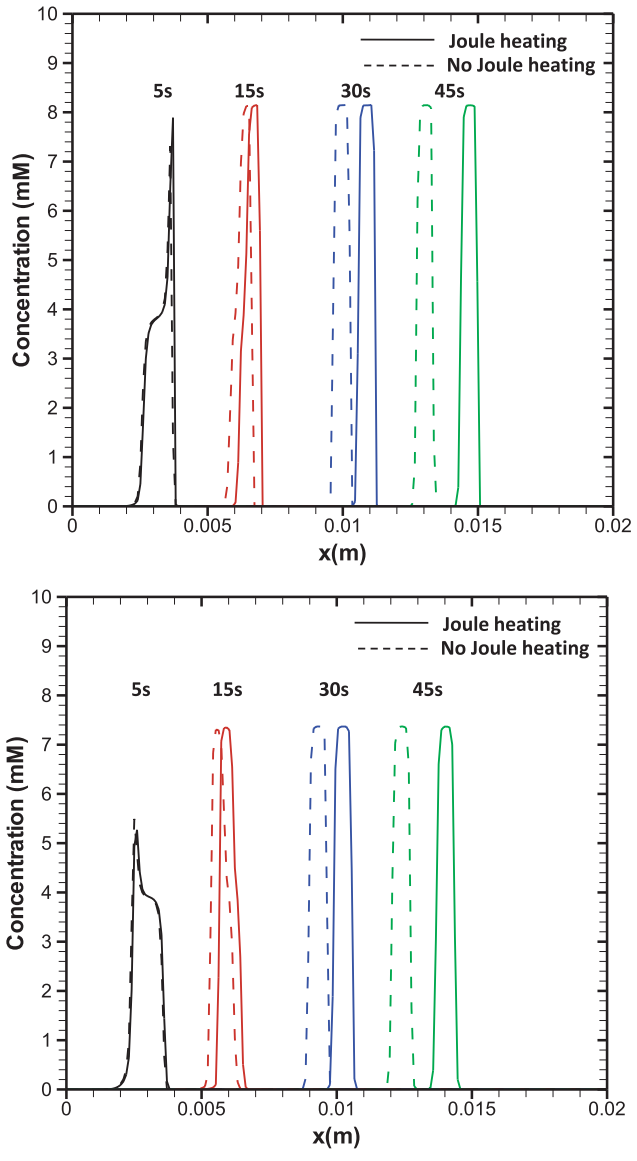

Fig. 5: Comparison of concentration profiles with and without considering Joule heating for (top) sample A and (bottom) sample B at different times. All other simulation conditions are same as in figure 4.

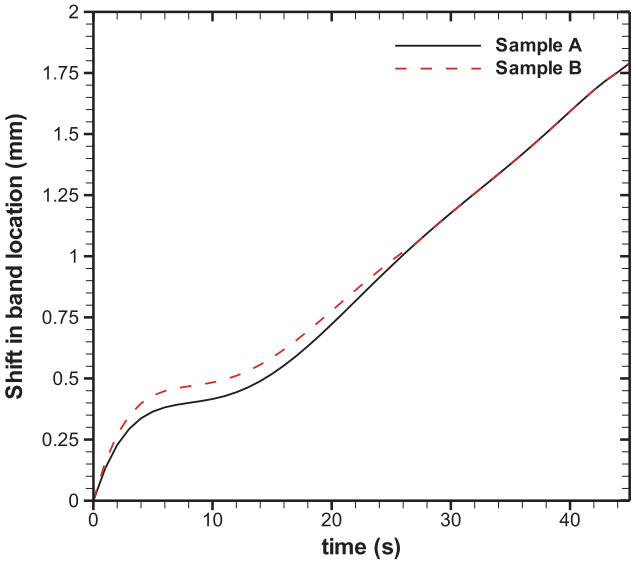

Fig. 6: Change in band position with time due to the Joule heating effect. All other simulation conditions are same as in figure 4.

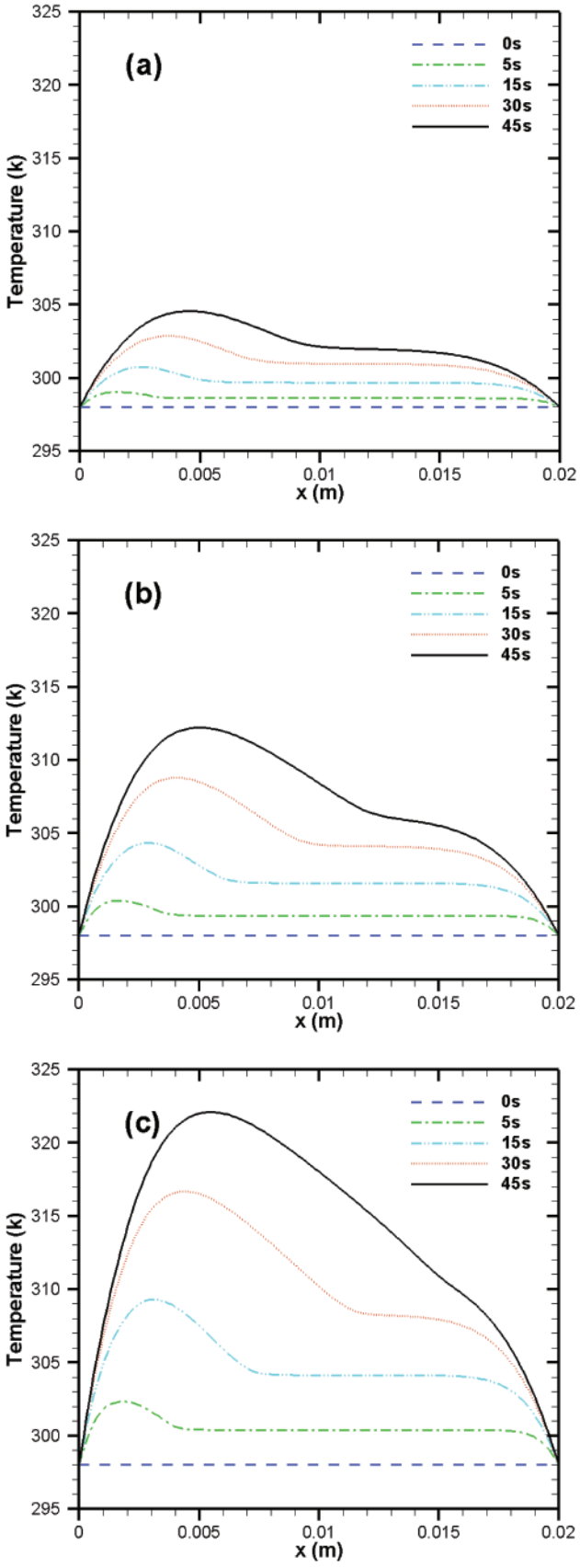

Fig. 7: Temperature distribution along the channel at different times for a nominal electric field of (a) 25 V/cm, (b) 37.5 V/cm, and (c) 50 V/cm.

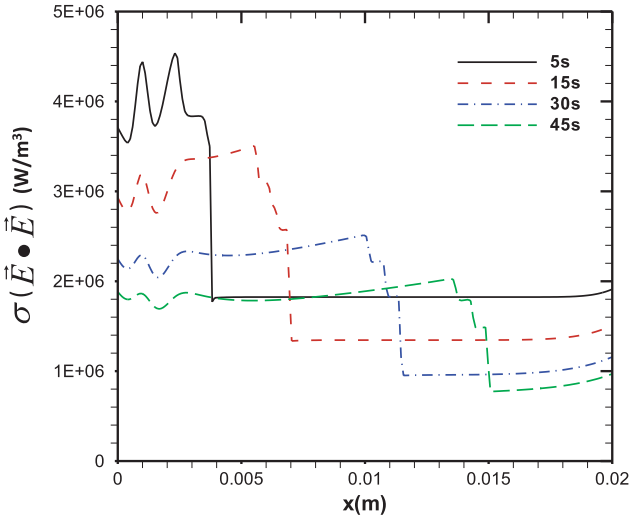

Fig. 8: Distribution of the heat generation term in the energy equation for a nominal electric field of 50 V/cm. All other simulation conditions are same as in Figure 4.

range (50 to 100 V) is based on recent experimental studies [17, 31], while the cathode is maintained at ground. It is possible to apply much higher applied electric field, but that is not desirable due to large Joule heating in the system. For all cases, temperature remains uniform at the beginning of the ITP process, but it becomes non-uniform very quickly due to the Joule heat generation in the system. The temperature peak takes place at the cathodic side (left). At 45 sec, the peak temperatures are 304 K, 312 K and 322 K for nominal electric field of 25 V/cm, 37.5 V/cm and 50 V/cm, respectively. The non-uniform temperature rise can be explained from the electric field and heat generation term (Figure 8). Unlike capillary electrophoresis, where a homogenous buffer is used, ITP takes place in a discontinuous buffer. Thus the electric field is the highest at the location of terminator where the conductivity is the lowest due to the presence of lowest mobility component in the system. On the other hand, the electric field is the lowest at the leader's location owing to the fact that only highest mobility component is present there. Hence, as shown in Figure 8, the volumetric heat generation is the highest in the cathodic side and the least in the anodic side for this anionic ITP. Moreover, the step-wise changes in heat generation at the interfaces are due to the changes in conductivity and electric field among various electrolytes and sample components.

For all three electric field cases (Figure 7), the temperature increases monotonically with time. This behavior is very similar to conduction heat transfer with locally varying generation term. In the absence of any bulk

flow term, the temperature remains highly nonuniform along the channel. As ITP progresses, the magnitude of generation term also changes. Since the terminator moves toward anode with time, heat generation also increases with time (Figure 8). It is noteworthy to mention that there is no active heat dissipation mechanism in the proposed system which makes this system even worse from thermal point of view. One can remove heat from the ITP system by introducing a highly (thermally) conductive flow chamber or applying a counter flow. The former case is not very common especially in microfluidic device, but the later solution is definitely achievable. As a matter of fact, in some ITP experiments, a counter flow is applied to keep the solute band at a particular location in the separation column [32]. Application of counter flow would be even more suitable for the microchannel ITP where the length of the channel is very short. However, this kind of back flow has not been very popular as dispersion takes place if a pressure driven parabolic flow is applied in the microchannel. The dispersion effect can be mitigated by applying a uniform countercurrent flow.

Figure 9(top) shows the temperature distribution in ITP with a uniform bulk (counter) flow for a nominal electric field of 50 V/cm. Since a uniform bulk flow is applied, there is no need to solve the Navier Stokes equations. Rather, in our numerical model, the constant bulk flow term is incorporated in the net flux term of the mass, charge and energy conservation equations. This bulk flow term also modifies the location of ITP band with time. In a recent study, Harrison and Ivory [32] reported that the counter flow can be used to immobilize the ITP band at a particular location in the channel. According to that study, the magnitude of bulk flow needed to immobilize the ITP band can be calculated as

$$v_{cf} = \frac{\mu_T \mu_L \Delta\phi}{L_L(\mu_L - \mu_T) - L_C \mu_L} \tag{10}$$

where L_C is the total length of the separation column, $\Delta\phi$ is the total nominal voltage across the separation channel, and μ_L and μ_T are absolute mobilities of leader and terminator, respectively. Thus, for the model input presented in table 1, the calculated counterflow velocity is 0.335 mm/s in a 2 cm long separation channel for a nominal potential drop of 100 V.

Figure 9(top) reveals that temperature decreases along the channel once a bulk flow is introduced in the ITP channel. There are two reasons for that. First, the bulk flow is responsible for an active convective cooling inside the ITP channel. Second, the bulk flow minimizes the amount of Joule heat generation in the system by restricting the movement of least conductive terminator in the downstream direction once the ITP reaches pseudo-steady state (Figure 9(bottom)). As seen from Figure 9(bottom), the terminator can move as much as 2.7 mm from the cathode reservoir when a bulk flow is applied. But the interface location between terminator and sample B moves downstream direction with time (Figure 4) if there is no countercurrent bulk flow in the system.

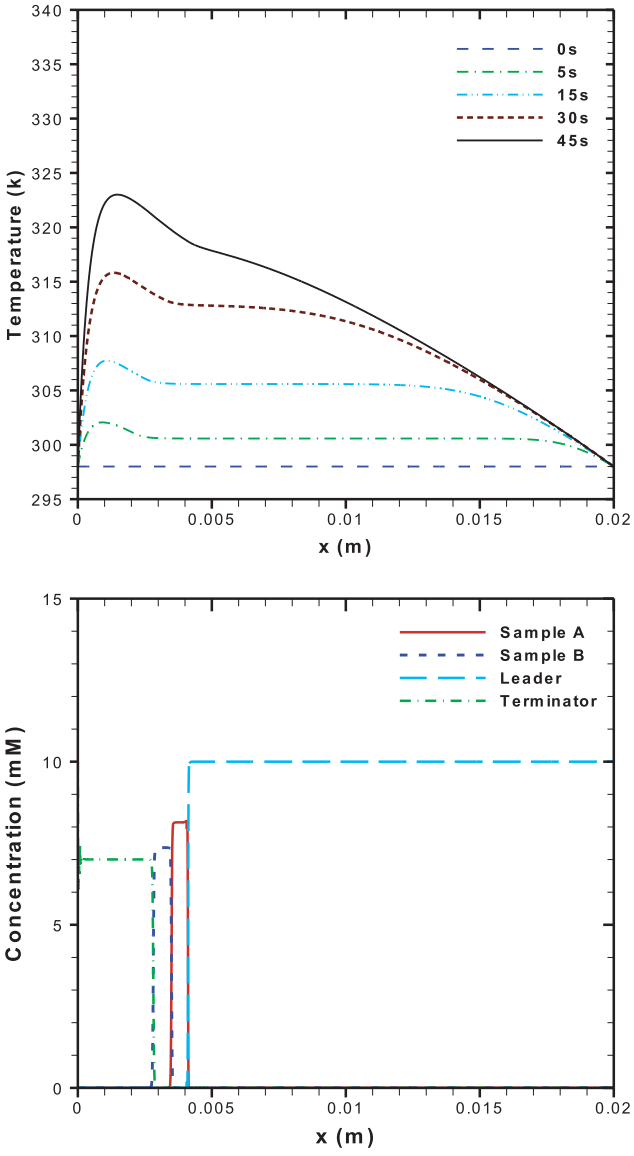

Fig. 9: (Top) Temperature distribution along the channel for an ITP with a countercurrent bulk flow. (Bottom) Steady state concentration distribution along the channel for case with a countercurrent bulk flow. Concentration results are presented for 45 sec as there is no significant changes in concentration after that. The bulk flow velocity is calculated as –0.335 mm/s. All other simulation conditions are same as in figure 4.

5 Conclusions

In this paper, temperature dependent ITP model is developed to study the effect of Joule heating on transient ITP separation behavior. The ITP model is based on mass, charge and energy conservation equations in addition to the electroneutrality condition. Using constant voltage mode anionic ITP, separation of two sample components are shown for cases with and without Joule heating. Numerical results show that the speed of band movements increases with time if the temperature contribution due to Joule heating is taken into consideration. Joule heating creates nonuniform temperature distribution along the channel where the peak temperature takes place at the interface of terminator and sample B. The buffer temperature increases monotonically with time if no countercurrent bulk flow is applied in the system. The counter flow can minimize the buffer temperature distribution in the separation channel, but the magnitude of peak temperature remains less affected by the countercurrent flow.

The amount of Joule heat generation depends on the concentration of ionic components in the system and the applied electric field. Hence, the Joule heating effect can be mitigated by decreasing the applied potential difference across the channel or applying a countercurrent bulk flow. The simulation results show that the temperature field remains transient. A steady state temperature distribution cannot be achieved unless an active cooling system is incorporated along the channel to extract the heat generated by the electric field driven Joule heating.

Acknowledgment

This work was supported by the National Research Foundation of Korea (NRF) grant funded by the Korea government (MEST) (No. 2012R1A1A2009392).

Received: August 19, 2011. Accepted: March 8, 2012.

References

[1] Holloway, C. J., and Battersby, R. V., 1984, "Preparative isotachophoresis," Methods in Enzymology, 104, pp. 281–301.

[2] Hirokawa, T., and Kiso, Y., 1994, "Preparative procedures in isotachophoresis," Journal of Chromatography A, 658(2), pp. 343–354.

[3] Kaniansky, D., Simunicova, E., Olvecka, E., and Ferancova, A., 1999, "Separations of enantiomers by preparative capillary isotachophoresis," Electrophoresis, 20(13), pp. 2786–2793.

[4] Jung, B., Bharadwaj, R., and Santiago, J. G., 2006, "On-chip millionfold sample stacking using transient isotachophoresis," Analytical Chemistry, 78(7), pp. 2319–2327.

[5] Bottenus, D., Jubery, T. Z., Ouyang, Y. X., Dong, W. J., Dutta, P., and Ivory, C. F., 2011, "10 000-fold concentration increase of the biomarker cardiac troponin I in a reducing union microfluidic chip using cationic isotachophoresis," Lab on a Chip, 11(5), pp. 890–898.

[6] Horiuchi, K., Dutta, P., and Hossain, A., 2006, "Joule-heating effects in mixed electro-osmotic and pressure-driven microflows under constant wall heat flux," Journal of Engineering Mathematics, 54(2), pp. 159–180.

[7] Chein, R. Y., Yang, Y. C., and Lin, Y. S., 2006, "Estimation of Joule heating effect on temperature and pressure distribution in electrokinetic-driven microchannel flows," Electrophoresis, 27(3), pp. 640–649.

[8] Kang, Y., Yang, C., and Huang, X., 2005, "Joule heating induced transient temperature field and its effects on electroosmosis in a microcapillary packed with microspheres," Langmuir, 21(16), pp. 7598–7607.

[9] Ge, Z. W., Yang, C., and Tang, G. Y., 2010, "Concentration enhancement of sample solutes in a sudden expansion microchannel with Joule heating," International Journal of Heat and Mass Transfer, 53(13–14), pp. 2722–2731.

[10] Huber, D., and Santiago, J. G., 2005, "Temperature gradient focusing in a microfluidic device," Journal of Heat Transfer-Transactions of the Asme, 127(8), pp. 806–806.

[11] Griffith, A., Catsimpoolas, N., and Kenney, J., 1973, "Analytical gel isotachophoresis of Proteins with carrier ampholyte spacers," Annals of the New york Academy of Sciences, 209, pp. 457–469.

[12] Masar, M., Zuborova, M., Bielcikova, J., Kaniansky, D., Johnck, M., and Stanislawski, B., 2001, "Conductivity detection and quantitation of isotachophoretic analytes on a planar chip with on-line coupled separation channels," Journal of Chromatography A, 916(1–2), pp. 101–111.

[13] Olvecka, E., Masar, M., Kaniansky, D., Johnck, M., and Stanislawski, B., 2001, "Isotachophoresis separations of enantiomers on a planar chip with coupled separation channels," Electrophoresis, 22(15), pp. 3347–3353.

[14] Reijenga, J. C., Verheggen, T., and Everaerts, F. M., 1985, "Theoretical and practical limitations of capillary isotachophoresis in trace analysis," Journal of Chromatography, 328(JUN), pp. 353–356.

[15] Gysler, J., Mazereeuw, M., Helk, B., Heitzmann, M., Jaehde, U., Schunack, W., Tjaden, U. R., and van der Greef, J., 1999, "Utility of isotachophoresis-capillary zone electrophoresis, mass spectrometry and high-performance size-exclusion chromatography for monitoring of interleukin-6 dimer formation," Journal of Chromatography A, 841(1), pp. 63–73.

[16] Pfeifer, P. A., Bonn, G. K., and Bobleter, O., 1983, "Determination of phenol in industrial-waste water by isotachophoresis," Fresenius Zeitschrift Fur Analytische Chemie, 315(3), pp. 205–207.

[17] Cui, H. C., Dutta, P., and Ivory, C. F., 2007, "Isotachophoresis of proteins in a networked microfluidic chip: Experiment and 2-D simulation," Electrophoresis, 28(7), pp. 1138–1145.

[18] Jung, B. G., Zhu, Y. G., and Santiago, J. G., 2007, "Detection of 100 aM fluorophores using a high-sensitivity on-chip CE system

and transient isotachophoresis," Analytical Chemistry, 79(1), pp. 345–349.
[19] Bottenus, D., Jubery, T. Z., Dutta, P., and Ivory, C. F., 2011, "10 000-fold concentration increase in proteins in a cascade microchip using anionic ITP by a 3-D numerical simulation with experimental results," Electrophoresis, 32(5), pp. 550–562.
[20] Krivtzun, V., Grass, B., Hergenroder, R., Bolshov, M., Niemax, K., and Zybin, A., 2001, "Temperature measurement of liquids by differential absorption of two diode lasers: Application of contactless optical detection in isotachophoresis," Applied Spectroscopy, 55(9), pp. 1251–1258.
[21] Koch, J., Zybin, A., and Niemax, K., 2002, "Narrow and broad band diode laser absorption spectrometry – concepts, limitations and applications," Spectrochimica Acta Part B-Atomic Spectroscopy, 57(10), pp. 1547–1561.
[22] Bier, M., Palusinski, O. A., Mosher, R. A., and Saville, D. A., 1983, "Electrophoresis – mathematical-modeling and computer-simulation," Science, 219(4590), pp. 1281–1287.
[23] Fidler, V., Vacik, J., and Fidler, Z., 1985, "Dynamics of isotachophoretic separation .1. Computer-simulation," Journal of Chromatography, 320(1), pp. 167–174.
[24] Mosher, R. A., Saville, D. A., and Thormann, W., 1992, The Dynamics of Electrophoresis, VCH, Weinheim.
[25] Deshmukh, R. R., and Bier, M., 1993, "Counterflow in isotachophoresis – computer-simulation and experimental studies," Electrophoresis, 14(3), pp. 205–213.
[26] Shim, J., Dutta, P., and Ivory, C. F., 2007, "Modeling and simulation of IEF in 2-D microgeometries," Electrophoresis, 28(4), pp. 572–586.
[27] Shim, J., Cho, M., and Dutta, P., 2011, "A method to determine quasi-steady state in constant voltage mode isotachophoresis," Electrophoresis, 32(9), pp. 988–995.
[28] Horiuchi, K., and Dutta, P., 2004, "Joule heating effects in electroosmotically driven microchannel flows," International Journal of Heat and Mass Transfer, 47(14–16), pp. 3085–3095.
[29] Shim, J., Dutta, P., and Ivory, C. F., 2007, "Finite-volume methods for isotachophoretic separation in microchannels," Numerical Heat Transfer Part a-Applications, 52(5), pp. 441–461.
[30] Hruska, V., Jaros, M., and Gas, B., 2006, "Simul 5 – Free dynamic simulator of electrophoresis," Electrophoresis, 27(5–6), pp. 984–991.
[31] Cui, H. C., Huang, Z., Dutta, P., and Ivory, C. F., 2007, "Automated electric valve for electrokinetic separation in a networked microfluidic chip," Analytical Chemistry, 79(4), pp. 1456–1465.
[32] Harrison, S. L. M., and Ivory, C. F., 2007, "Prediction of the location of stationary steady-state zone positions in counterflow isotachophoresis performed under constant voltage in a vortex-stabilized annular column," Journal of Separation Science, 30(18), pp. 3255–3261.
[33] Weast, R., Astle, M. J., and Beyer, W. H., 1986, CRC Handbook of Chemistry and Physics, CRC Press Inc., Boca Raton, FL.
[34] Tang, G., and Yang, C., 2008, Numerical modeling of Joule heating induced temperature gradient focusing in microfluidic channels, Electrophoresis, 29, pp. 1006–1012.